Direct Identification of the $C_2H(X^2\Sigma^+) + O(^3P) \rightarrow CH(A^2\Delta) + CO$ Reaction as the Source of the $CH(A^2\Delta \rightarrow X^2\Pi)$ Chemiluminescence in $C_2H_2/O/H$ Atomic Flames

Katia Devriendt and Jozef Peeters*

Department of Chemistry, University of Leuven, Celestijnenlaan 200F, B-3001 Leuven, Belgium

Received: October 31, 1996; In Final Form: January 28, 1997[⊗]

In this work, the intensity of the $CH(A^2\Delta)$ chemiluminescence, $I(CH^*)$, as well as the concentrations of ground state C_2H radicals and O atoms were measured as a function of the reaction time in a variety of helium-diluted $C_2H_2/O/H$ mixtures in an isothermal flow reactor at temperatures of 290, 410, 520, 590, 675, and 925 K and at a total pressure of 2 Torr. The species concentrations [O] and [C_2H] were measured using molecular beam sampling−threshold ionization mass spectrometry (MB-TIMS). At each temperature, the intensity $I(CH^*)$ was found to be directly proportional to the [C_2H][O] concentration product, over a range of two decades, irrespective of the initial mixture composition or the reaction time. Using the $NO + O \rightarrow NO_2^*$ chemiluminescence as a calibration standard, CH* formation rates were derived from the measured $I(CH^*)$, and the values of the rate coefficient k_{2a} of the CH*-forming reaction channel $C_2H + O \rightarrow CH(A^2\Delta) + CO$ (r2a) were thus derived from the slopes of the $I(CH^*)$ versus [C_2H][O] plots. The results, for 290 K $< T <$ 925 K, can be represented by the Arrhenius expression $k_{2a} = 2.4 \times 10^{-11} \exp[-230/T(K)]$ cm^3 molecule^{-1} s^{-1}; the possible systematic error is a factor of 2, due to the uncertainty of the C_2H calibration factor. The value at 290 K, 1.1×10^{-11}, is in fair agreement with our recent result obtained in an independent pulse laser photolysis/chemiluminescence experiment. The addition of methane was found to suppress $I(CH^*)$ in quantitative agreement with the C_2H formation mechanism in $C_2H_2/O/H$ systems elucidated earlier by us. It is argued that the fast reaction r2a is a major if not the dominant CH* source also in hot hydrocarbon flames.

Introduction

The intense blue chemiluminescence around 430 nm is one of the most characteristic features of hydrocarbon flames. Already 35 years ago, Bass and Broida[1] unambiguously identified this emission as the (0,0) band of the $CH(A^2\Delta \rightarrow X^2\Pi)$ transition, but the (chemical) process responsible for the formation of the excited CH* has not yet been definitely established.

The reaction proposed by Gaydon,[2]

$$C_2(X'^3\Pi) + OH(X^2\Pi) \rightarrow CH(A^2\Delta) + CO \qquad (r1)$$

was supported by Bulewicz et al.,[3] who found that the quotient [CH*]/[C_2][OH] in hot low-pressure C_2H_2/O_2 flames was independent of several flame parameters, within ∼25%. However, some years later Brenig[4] showed that there is no production of CH* in systems containing C_2, CH, and OH in their electronic ground state without atomic oxygen being present. The essential role of O atoms in the production of CH*, demonstrated by Brenig, supports the reaction of ground state ethynyl radicals with O atoms,

$$C_2H(X^2\Sigma^+) + O(^3P) \rightarrow CH(A^2\Delta) + CO \qquad (r2a)$$

$$\rightarrow \text{other products} \qquad (r2b)$$

which had been suggested earlier by Glass et al.[5] and by Brennen and Carrington.[6]

Grebe and Homann[7] investigated the strong CH* emission of room-temperature $C_2H_2/O/H$ atomic flames. Concurring with Brenig, they ruled out Gaydon's reaction because, at the very low OH concentrations in such systems, extremely high C_2 concentrations would be required to explain the high observed CH* production. On the other hand, on the basis of the measured O concentrations and C_2H concentrations calculated from an assumed reaction mechanism, they could explain the observed CH* by reaction r2a when adopting a channel rate coefficient k_{2a} of 1.1×10^{-12} cm^3 molecule^{-1} s^{-1}. However, Joklik et al.[8] needed a k_{2a} value an order of magnitude higher to account for the intense CH* emission of C_2H_2/O_2 flames by reaction r2a.

Renlund et al.[9] suggested the reaction of C_2H with molecular rather than atomic oxygen as a source of CH* chemiluminescence:

$$C_2H(X^2\Sigma^+) + O_2 \rightarrow CH(A^2\Delta) + CO_2 \qquad (r3a)$$

$$\rightarrow \text{other products} \qquad (r3b)$$

Besides the above, several other processes, including energy exchange mechanisms, have been proposed to explain the CH* emission of hydrocarbon flames; they have been briefly reviewed by Becker and Wiesen.[10]

Very recently, in a pulse laser photolysis/chemiluminescence study,[11] we performed a direct determination of the rate constants of the $CH(A^2\Delta)$-forming reactions r2a and r3a, obtaining $k_{2a} = (1.8 \pm 0.7) \times 10^{-11}$ and $k_{3a} = (3.6 \pm 1.4) \times 10^{-14}$ cm^3 molecule^{-1} s^{-1}, respectively, at $T = 290$ K. The unexpectedly high rate constant of reaction channel r2a indicates that this reaction is a very likely source of CH* in hydrocarbon combustion/oxidation systems. Fuel-rich hydrocarbon flames in general contain sizeable amounts of C_2H, as is witnessed by the presence of C_4H_2,[12] which is well-known to be formed via the reaction between C_2H and C_2H_2. At higher temperatures, C_2H may arise by H-abstraction from C_2H_2 by OH and H; recently we obtained indirect evidence[13] that the reaction with H at temperatures near 2000 K is more than an order of magnitude faster than hitherto accepted and—notwithstanding its activation energy of 30 kcal/mol—can produce significant

* Author to whom correspondence should be addressed.

⊗ Abstract published in *Advance ACS Abstracts,* March 15, 1997.

S1089-5639(96)03434-2 CCC: $14.00

amounts of C_2H in fuel-rich flames. At low temperatures, on the other hand, where the endoergic direct H-abstraction processes are too slow, another C_2H formation mechanism, initiated by the $C_2H_2 + O$ reaction, is operative. This mechanism was recently identified and characterized by us in He-diluted C_2H_2/O/H atomic flames at temperatures $T \approx 600$ K:[14]

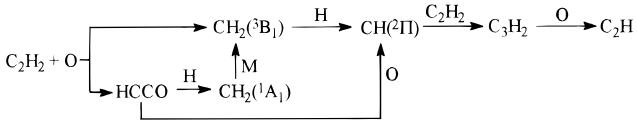

All the reactions subsequent to the primary reaction are very fast, such that the mechanism, despite its complexity, is an efficient C_2H source.

In light of the above, we set out in the present work to verify directly whether the reaction between ground state C_2H radicals and O atoms is indeed responsible for the CH* chemiluminescence in acetylene flames. In this study, we opted for an investigation of C_2H_2/O/H atomic flame systems over an extended temperature range of 300−1000 K. Such systems offer the excellent spatial resolution that is highly desirable for such a verification.

Experimental Section

The experimental arrangement used in this investigation consists basically of a conventional isothermal fast-flow reactor, coupled to a molecular beam sampling−threshold ionisation mass spectrometer (MB-TIMS); it has been described on several occasions already,[14,15] and only its major characteristics will be repeated here briefly.

The flow reactor consists of a cylindrical quartz tube (i.d. = 16.5 mm) equipped with a discharge side arm, an axially movable central injector tube, and an additional side inlet to admit carrier gas. Oxygen and hydrogen atoms were generated by dissociation of O_2 and H_2, diluted in He, in a 75 W microwave discharge. Acetylene—also diluted in He—was added through the central injector tube. The reactor was treated with a 10% HF solution to suppress radical loss on the reactor walls. The reactor tube is equipped with a heating mantle, allowing uniform reactor temperatures up to 1000 K.

Quantitative and qualitative analysis of the relevant species in the investigated C_2H_2/O/H atomic flames was achieved by MB-TIMS. The gas at the reactor exit was sampled through a 0.3 mm pinhole in a quartz cone giving access to the first of two differentially pumped low-pressure chambers. After mechanical modulation—to allow phase sensitive detection—the resulting molecular beam enters the second low-pressure chamber, which houses the electron-impact ionizer and an Extranuclear quadrupole mass spectrometer. A lock-in amplifier was used to distinguish between the beam and background ions.

Concentration-versus-time profiles of the primary reactants C_2H_2, O, and H were recorded at electron energies only a few electronvolts (eV) above the respective ionization potentials, in order to suppress signal contamination by fragment ions. O_2 was ionized at an electron energy of 70 eV. The C_2H signals were monitored at a nominal electron energy of 14 eV, where the signal to noise ratio proved to be optimal; the C_2H signals were duly corrected for the C_2H^+ fragment ion contribution from C_2H_2. The state of the C_2H involved is the $X\ ^2\Sigma^+$ ground state, as follows from the experimental ionization potential of 11.7 ± 0.4 eV.[14]

Absolute concentrations of the molecules C_2H_2, O_2, H_2, and also NO and CH_4, used in additional experiments, were derived from the measured (fractional) flows of certified high-purity gases and from the total pressure. The absolute concentrations of O and H atoms were determined by partial dissociation of O_2 and H_2, respectively, in the microwave discharge and application of the discharge on/off method.[15]

The $CH(A^2\Delta \rightarrow X^2\Pi)$ chemiluminescence at the reactor exit was collected by a lens and focused through an Oriel narrow-bandpass interference filter (429.5 ± 4 nm) onto a Hamamatsu 1P28 photomultiplier.

All experiments were carried out at a total pressure of 2 Torr (≥98% He) and at temperatures between 290 and 925 K. Depending on temperature, the linear flow velocities ranged from 20 to 63 m s^{-1}, and the associated maximum reaction times from 11.0 to 3.5 ms. Gases and mixtures, used without further purification, were He (99.9996%) as discharge-inlet carrier gas, He (99.994%) as additional carrier gas, CH_4 (99.95%) (all L'Air Liquide), and certified 1%-10% mixtures of C_2H_2 (99.6%), O_2 (99.998%), H_2 (99.999%), and NO (99.96%) in UHP He (all UCAR).

Results

To ascertain first that the observed blue chemiluminescence of the investigated C_2H_2/O/H atomic flames can be fully assigned to the $CH(A^2\Delta,v'=0) \rightarrow CH(X^2\Pi,v''=0)$ transition, the collected and focused luminescence was dispersed with a 0.22 m SPEX double-grating monochromator. The features of the recorded spectrum in the 420−450 nm region are clearly identifiable as those of the (0,0) band of the $CH(A^2\Delta \rightarrow X^2\Pi)$ emission spectrum, with the band origin at 431.5 nm; the rotational structure fully agrees with the emission data of Bass and Broida.[1]

1. Linear Relation Between *I*(CH*) and *i*(C_2H)[O]. Our primary objective was to verify directly whether the $C_2H(X^2\Sigma^+) + O(^3P) \rightarrow CH(A^2\Delta) + CO$ reaction is indeed the dominant CH* source. If so, the measured CH* emission signal of the (0,0) band, *I*(CH*), at a given temperature, should be directly proportional to the product of the mass spectrometric signal of C_2H and the O atom concentration, *i*(C_2H)[O], irrespective of the initial mixture composition and of the reaction time.

Indeed, for quasi-steady state conditions of CH*, which disappears very rapidly by radiative decay

$$CH(A^2\Delta) \rightarrow CH(X^2\Pi) + h\nu \qquad (k_r)$$

and by collisional quenching,

$$CH(A^2\Delta) + Q \rightarrow CH(X^2\Pi) + Q \qquad (k_q)$$

$$\rightarrow \text{products}$$

one can write

$$I(CH^*) = b[CH^*]_{ss}k_r f(0,0) = bU_f(CH^*)\frac{k_r}{k_r + \Sigma k_q[Q]} f(0,0) \quad (1)$$

where *I*(CH*) is the measured CH* emission signal of the (0,0) band; $[CH^*]k_r f(0,0) \equiv E(CH^*)$ is the CH*(0,0) band photon emission rate, i.e. the number of photons emitted per unit time and unit volume; *b* is the instrumental proportionality factor between the signal *I*(CH*) and the emission rate *E*(CH*); U_f(CH*) is the formation rate of $CH(A^2\Delta,v'=0)$; $k_r/(k_r + \Sigma k_q[Q])$ is the CH* emission yield; and *f*(0,0) is the fraction of CH* emission in the (0,0) band.

In practice, the quasi-steady state will always be established in our experiments because the 0.5 μs lifetime of the CH* intermediate is several orders of magnitude shorter than the

TABLE 1: Initial Composition (in 10^{14} molecules cm^{-3}) of the Investigated Mixtures at $T = 290-925$ K and $p = 2$ Torr (He Bath Gas)

mixture	temp (K)	$[C_2H_2]_0$	$[O]_0$	$[H]_0$	$[O_2]_0$	$[H_2]_0$
1a	590	1.26	1.58	0.00	0.86	0.00
1b	590	1.26	1.58	0.47	0.89	0.59
1c	590	1.26	1.58	0.95	0.94	1.10
1d	590	1.26	1.58	1.26	0.98	1.31
1e	590	1.26	1.58	1.58	1.17	1.55
1f	590	1.26	1.58	1.90	1.47	1.76
1g	590	1.26	1.58	2.31	1.70	2.00
1h	590	1.26	1.58	2.53	2.15	2.04
2	590	1.31	2.45	1.25	2.19	1.13
3	590	1.36	2.34	1.51	1.98	1.48
4	590	1.36	1.62	1.23	1.92	1.31
5	290	2.67	4.03	1.97	3.22	2.18
6a	290	1.98	2.73	2.28	4.16	2.19
6b	290	1.98	2.73	2.28	5.79	2.19
6c	290	1.98	2.73	2.28	6.66	2.19
6d	290	1.98	2.73	2.28	8.05	2.19
6e	290	1.98	2.73	2.28	9.39	2.19
6f	290	1.98	2.73	2.28	11.60	2.19
7	410	1.98	2.62	1.56	2.89	1.52
8	520	1.58	2.57	1.03	2.45	1.17
9	675	1.24	2.13	0.56	1.82	0.70
10	925	1.05	2.03	0.53	2.50	0.75

millisecond time scale for significant concentration changes of CH*. Also, in our conditions, the CH* emission yield is very close to unity and therefore constant, as found from the following. Becker et al.[16] and Bauer et al.[17] reported radiative lifetimes of electronically excited CH($A^2\Delta,v'=0$) radicals of 537 $\pm$ 5 and 526 $\pm$ 11 ns, respectively. The former also found He to be an inefficient quencher of the CH* emission; they determined a rate constant for quenching by He of $(6.8 \pm 2.0) \times 10^{-14}$ cm^3 molecule^{-1} s^{-1} at 297 K. Other possible quenchers of CH* in our systems are C_2H_2, O_2, H_2, O, and H atoms. Becker and Wiesen[10] measured the rate constants for removal of CH* by these different reactants and obtained the following 297 K values (in units of cm^3 molecule^{-1} s^{-1}): $k(C_2H_2) = 1.6 \times 10^{-10}$, $k(O_2) = 1.1 \times 10^{-11}$, $k(H_2) = 1.1 \times 10^{-11}$, $k(O) \leq 2.0 \times 10^{-10}$, and $k(H) = 1.7 \times 10^{-10}$. The removal of CH* by these reactions can involve both collisional deactivation to the electronic ground state and chemical reaction. Using these values, one calculates that the $\Sigma k_q[Q]$ value in our conditions is in the range $(2-4) \times 10^4$ s^{-1}, which is negligible compared to the k_r value of $\sim 2 \times 10^6$ s^{-1}. Thus, the CH* emission yield is ≥ 0.98. The ratio of the Einstein coefficients for the (0,1) and (0,0) bands of the CH(A$\rightarrow$X) transition is 0.018 ± 0.002,[18] such that the fraction $f(0,0)$ in eq. 1 is almost unity.

Therefore, if CH* arises by the $C_2H + O$ reaction, one should have a linear relationship between I(CH*) and the product of the relative C_2H concentration $i(C_2H)$ and the O atom concentration:

$$I(\mathrm{CH}^*) = (k_{2a}b/S_{C_2H})i(C_2H)[O] \qquad (2)$$

where k_{2a} is the rate constant of reaction r2a, b the proportionality factor between I(CH*) and E(CH*), and $S_{C_2H} \equiv i(C_2H)/[C_2H]$ the MB-TIMS sensitivity for C_2H; the overall proportionality factor $c \equiv k_{2a}b/S_{C_2H}$ can only be a function of temperature.

This proportionality was verified first in 11 different reaction mixtures at $T = 590$ K, for reaction times t varying from 0.9 to 5.2 ms. The initial mixture compositions are listed in Table 1. In these mixtures, the concentrations of C_2H, O, H, and O_2 varied over factors of 13.4, 9.8, 7.4, and 2.8, respectively, while the CH* emission intensity spanned a range of 2 orders of magnitude. As an example, concentration versus time profiles of the initial reactants and of the intermediates C_2H and CH* in mixture 2 are shown in Figure 1.

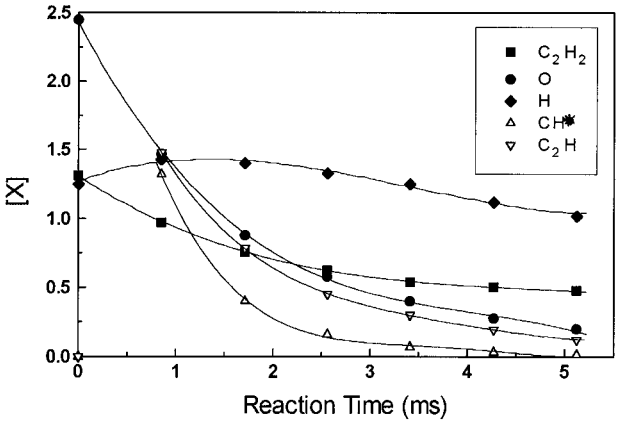

Figure 1. Concentration versus time profiles of C_2H_2, O, H, C_2H, and CH* in C_2H_2/O/H mixture 2 at $T = 590$ K. The absolute concentration of CH* was derived from the emission signal I(CH*). For X = C_2H_2, O, and H: units of 10^{14} molecule cm^{-3}. X = CH*: units of 10^7 molecule cm^{-3}. X = C_2H: units of 10^{10} molecule cm^{-3}. Curves are polynomial fits.

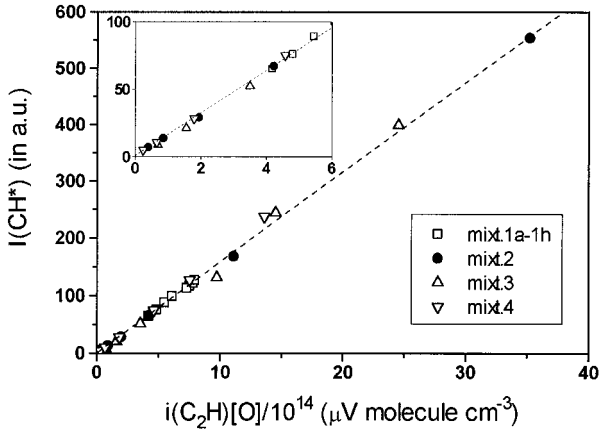

Figure 2. Plot of the CH* emission signal I(CH*) (in au = arbitrary units) versus the concentration product $i(C_2H)[O]$ for the investigated C_2H_2/O/H atomic flames at $T = 590$ K. Bottom left side of the plot magnified in inset.

The plot of eq 2, displayed in Figure 2, demonstrates the near-perfect linear relationship between I(CH*) and $i(C_2H)[O]$, fully consistent with the $C_2H(X^2\Sigma^+) + O(^3P) \rightarrow CH(A^2\Delta) + CO$ reaction as the CH* formation route in the investigated C_2H_2/O/H atomic flames.

The linear relation between the CH* emission signal and the $i(C_2H)[O]$ product was verified for various temperatures, in the 290$-$925 K range. At each temperature, several mixtures were investigated; data were always obtained over the full reaction time span, which varies from 11.0 ms at 290 K to 3.5 ms at 925 K. Table 1 summarizes the initial mixture compositions. The various plots of I(CH*) versus $i(C_2H)[O]$, at temperatures of 290, 410, 520, 590, 675, and 925 K, are displayed in Figure 3. For each temperature, the CH* emission signal is seen to be directly proportional to $i(C_2H)[O]$ over the entire time span and for all mixtures. This establishes the $C_2H(X^2\Sigma^+) + O(^3P) \rightarrow CH(A^2\Delta) + CO$ reaction as the CH* formation route in the investigated C_2H_2/O/H atomic flames at all temperatures.

It should be noted that in the 290 K mixtures 6a-6f, the O_2 concentration was gradually increased by admitting additional O_2 via a separate inlet, whereas the initial concentrations of C_2H_2 and O were kept constant. Table 2 shows the concentrations of O, O_2, and C_2H together with the CH* emission intensities at an identical reaction time of 3 ms; the products $i(C_2H)[O]$ and $i(C_2H)[O_2]$ at $t = 3$ ms, normalized to their values in mixture 6a, are also tabulated. If the $C_2H(X^2\Sigma^+) + O_2 \rightarrow CH(A^2\Delta) + CO_2$ reaction were to be an important CH* source,

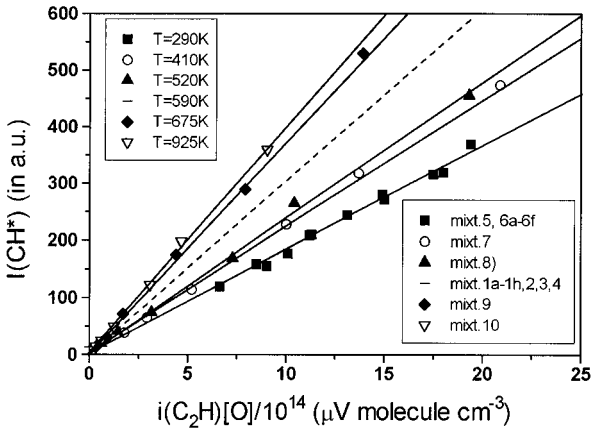

Figure 3. Plot of I(CH*) (in au = arbitrary units) versus the product $i(C_2H)[O]$ for C_2H_2/O/H atomic flames at $T = 290$, 410, 520, 590, 675 and 925 K. For reasons of clarity the I(CH*) values have been multiplied by 1.0, 1.2, 1.5, 1.8, 2.0, and 2.4, respectively. Data at 590 K represented by linear regression line (- - -) (see Figure 2).

TABLE 2: Impact of O_2 Addition on the Relative CH* and C_2H Concentrations in Mixtures 6a−6f after 3.0 ms Reaction Time (T = 290 K)

mixture	$[O]^a$	$[O_2]^a$	C_2H^b	CH* ^{b}	$i(C_2H)[O]^b$	$i(C_2H)[O_2]^b$
6a	2.73	4.10	1.00	1.00	1.00	1.00
6b	2.73	5.72	0.85	0.84	0.85	1.16
6c	2.73	6.61	0.74	0.76	0.74	1.17
6d	2.73	7.99	0.62	0.65	0.62	1.21
6e	2.73	9.32	0.58	0.55	0.58	1.27
6f	2.73	11.0	0.51	0.49	0.51	1.34

^{a} Concentrations in units of 10^{14} molecules cm^{-3}. ^{b} Values normalized to those of mixture 6a.

one would expect higher CH* signals upon increasing $[O_2]$. The experiment reveals an opposite effect: [CH*] is not proportional to the $i(C_2H)[O_2]$ product at all; rather, the addition of molecular oxygen to the system suppresses the CH* radiation. Moreover, $[C_2H]$ also decreases, in parallel with [CH*]. Since the O atom concentration remains nearly unchanged, the only straightforward explanation is that C_2H—being the precursor radical for CH* formation via reaction r2a—is removed rapidly by O_2, leading mainly to products other than CH* + CO_2. Van Look et al.[19] and Opansky et al.[20] measured a value of 3.3×10^{-11} cm^3 molecule^{-1} s^{-1} for the total $C_2H + O_2$ rate constant at 295 K. Recently, we found that the $CH(A^2\Delta)$ yield of this reaction is only $\sim 1.1 \times 10^{-3}$.[11]

2. Absolute Determination of k_{2a}. As shown above, the rate constant k_{2a} of the now established CH* source in C_2H_2/O/H atomic flames

$$C_2H(X^2\Sigma^+) + O(^3P) \rightarrow CH(A^2\Delta) + CO \qquad \text{(r2a)}$$

at a given temperature equals the slope of the straight line in the corresponding I(CH*) versus $i(C_2H)[O]$ plot, multiplied by the (T-dependent) constant S_{C_2H}/b.

The instrumental sensitivity of the MB-TIMS apparatus for C_2H, S_{C_2H}, was assumed to be equal to $S_{C_2H_2}$ at an identical excess ionizing electron energy above the respective ionization potentials and under the same experimental conditions; the expected error is a factor of $\sim$2. The T-dependence of S_{C_2H} was likewise taken the same as that of $S_{C_2H_2}$.

The measured CH* chemiluminescence signal, I(CH*), can be converted into the photon emission rate E(CH*) on the basis of the measured signal $I(NO_2^*)$ for the well-characterized reference reaction[21]

$$NO + O \rightarrow NO_2^* \xrightarrow{M} NO_2 + h\nu \qquad \text{(r4)}$$

TABLE 3: Rate Coefficient k_{2a} Determined at T = 290−925 K and Associated Statistical 2σ Error Margins

T (K)	k_{2a} (cm^3 molecule^{-1} s^{-1})	T (K)	k_{2a} (cm^3 molecule^{-1} s^{-1})
290	$(1.10 \pm 0.12) \times 10^{-11}$	590	$(1.48 \pm 0.15) \times 10^{-11}$
410	$(1.44 \pm 0.15) \times 10^{-11}$	675	$(1.85 \pm 0.18) \times 10^{-11}$
520	$(1.66 \pm 0.16) \times 10^{-11}$	925	$(1.92 \pm 0.18) \times 10^{-11}$

The NO_2* chemiluminescence is ideally suited as a quantitative standard because (i) it appears as a continuous spectrum from 400 to 1400 nm and (ii) the emission rate is independent of the total pressure in the 0.5−10 Torr range and is directly proportional to the concentration product [NO][O]. Fontijn et al.[21] determined the absolute total rate constant k_4 at room temperature: $k_4 = (6.4 \pm 1.9) \times 10^{-17}$ cm^3 molecule^{-1} s^{-1}.

We can write

$$E(\text{CH*}) = I(\text{CH*})\frac{E(NO_2^*)b_{NO_2^*}}{I(NO_2^*)\, b_{\text{CH*}}}$$

with the photon emission rate $E(NO_2^*)$ given by the known product k_4[NO][O]. The respective $b_i \equiv I_i^*/E_i^*$ are found from the measured or known spectral distributions of the emissions $E_n(\lambda)$, convoluted by the transmission curves $\text{Tr}_f(\lambda)$ of the respective filters and the spectral response $R(\lambda)$ of the photomultiplier:

$$\frac{I_i^*}{E_i^*} = \frac{g\int E_n(\lambda)\, \text{Tr}_f(\lambda)\, R(\lambda)\, \text{d}\lambda}{\int E_n(\lambda)\, \text{d}\lambda}$$

Since one needs only the ratio $b_{NO_2^*}/b_{\text{CH*}}$ and since the two measurements were carried out in exactly identical conditions, the geometrical photon collection factor g cancels.

The spectral distribution of the CH* emission $E_n(\lambda)$(CH*) broadens somewhat with increasing temperature due to the population of higher rotational states. As a result, the relative integrated transmission through the Oriel narrow-bandpass interference filter decreases by 20 ± 10% from 290 to 925 K. This small and rather uncertain change was not taken into account.

The $I(NO_2^*)$ reference emission intensities and the corresponding [NO] and [O] were monitored in an NO/O mixture diluted in He, with O atoms also created by partial dissociation of O_2, under exactly identical instrumental conditions as the CH* experiments. A Schott OG570 long wave pass filter ($\lambda >$ 570 nm) was used here instead of the narrow-bandpass interference filter of the CH* experiments.

The resulting k_{2a} values at each temperature are listed in Table 3 and displayed in Figure 4; they can be fitted by the following Arrhenius equation for the temperature range $T = 290-925$ K:

$$k_{2a} = (2.4 \pm 0.3) \times 10^{-11} \exp[-(230 \pm 75)/T(\text{K})]$$
$$\text{cm}^3\ \text{molecule}^{-1}\ \text{s}^{-1}$$

The probable systematic error is estimated to be a factor of $\sim$2, due largely to the expected uncertainty of the MB-TIMS calibration factor for C_2H. It should be understood that k_{2a} is the rate constant for formation of $CH(A^2\Delta, v'=0)$; it cannot be excluded that there could be production of CH* in higher vibrational states.

3. Effect of CH_4 Addition on the CH* Production. Relying on the fact that the key intermediates $CH(X^2\Pi)$ and $CH_2(^1A_1)$ are the only species in C_2H_2/O/H systems that are highly reactive toward methane,[22−27] a supplementary experiment was performed that should allow a quantitative validation of the overall CH* formation mechanism. Both $CH(X^2\Pi)$ and $CH_2(^1A_1)$ possess the unique combination of a lone pair and a

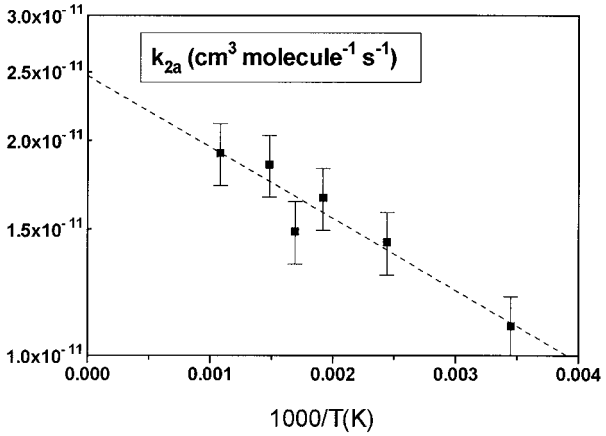

Figure 4. Arrhenius plot of the rate constant k_{2a} of the reaction channel $C_2H(X^2\Sigma^+) + O(^3P) \rightarrow CH(A^2\Delta) + CO$. Error bars indicate the statistical 2σ margins.

TABLE 4: Impact of CH_4 Addition on the Relative CH* Concentrations in a C_2H_2/O/H Mixture after 3.0 ms Reaction Time (T = 290 K); Comparison with the Calculated CH*, $CH(X^2\Pi)$, $CH_2(^1A_1)$, and C_2H Concentrations

$[CH_4]^a$	$[CH^*]_{exp}{}^b$	$[CH^*]_{calc}{}^b$	$[CH(X^2\Pi)]_{calc}{}^b$	$[CH_2(^1A_1)]_{calc}{}^b$	$[C_2H]_{calc}{}^b$
0	1.00	1.00	1.00	1.00	1.00
9.3	0.60	0.56	0.58	0.87	0.56
17.0	0.42	0.40	0.42	0.79	0.40
26.0	0.29	0.29	0.31	0.71	0.29
33.0	0.26	0.24	0.26	0.66	0.23

[a] Methane concentration in units of 10^{14} molecule cm^{-3}. [b] Concentrations are normalized to CH_4-free values.

vacant p orbital, which allows a fast insertion into the C−H bond of the CH_4 molecule. Hence, addition of CH_4 will selectively scavenge the $CH_2(^1A_1)$ and $CH(X^2\Pi)$ radicals. As a result, the formation of CH* via the sequences

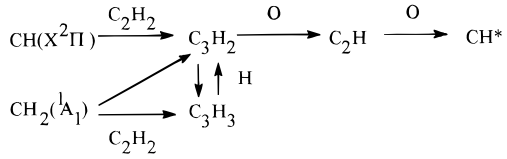

should be inhibited.

This experiment was carried out at room temperature, where reactions of CH_4 with the reactants O and H and with other intermediates in C_2H_2/O/H systems are still negligibly slow. The initial mixture composition was $[C_2H_2]_0 = 2.50 \times 10^{14}$, $[O]_0 = 2.72 \times 10^{14}$, $[H]_0 = 3.40 \times 10^{14}$, and $[O_2]_0 = 4.80 \times 10^{14}$ molecule cm^{-3}. In this mixture, relative concentrations of CH* were monitored upon the substitution of increasing amounts of He bath gas by CH_4, always at a reaction time of 3.0 ms. The CH_4 concentrations ranged from 9.3×10^{14} to 3.3×10^{15} molecules cm^{-3}. It was ascertained that no sensitivity decrease was induced due to CH_4 addition. The results are shown in Table 4. The listed relative CH* concentrations are normalized to the signal strengths in CH_4-free conditions. A very sharp reduction of [CH*] is observed upon substituting increasing amounts of He by CH_4; at the maximum $[CH_4]$ of 3.3×10^{15} molecules cm^{-3} only ~25% of the original CH* concentration is left. Although CH_4 is an effective CH* quencher—Bauer et al.[17] determined a rate constant of 2.2×10^{-11} cm^3 molecules^{-1} s^{-1} at room temperature—the CH* + CH_4 reaction can reduce [CH*] by only 3.8% at most, since radiative decay remains by far the dominant CH* destruction route. Therefore, the only plausible explanation for the strong decrease of [CH*] upon CH_4 substitution is that it removes the precursors $CH(X^2\Pi)$ and $CH_2(^1A_1)$.

This was verified quantitatively by kinetic modeling calculations. The acetylene oxidation mechanism is well-characterized at room temperature.[28] The following reactions were added to the reaction mechanism:

$$CH_2(^1A_1) + CH_4 \rightarrow 2CH_3 \qquad k = 6.0 \times 10^{-11}\ ^{23-25}$$

$$\rightarrow CH_2(^3B_1) + CH_4 \quad k = 1.2 \times 10^{-11}$$

$$CH(X^2\Pi) + CH_4 \rightarrow C_2H_4 + H \qquad k = 8.4 \times 10^{-11}\ ^{26,27}$$

$$C_2H + CH_4 \rightarrow \text{products} \qquad k = 3.0 \times 10^{-12}\ ^{29}$$

(rate constants k in units of cm^3 molecule^{-1} s^{-1}). In Table 4 the calculated [CH*] reduction is compared with the experimental [CH*] reduction. Table 4 also lists the calculated $CH(X^2\Pi)$, $CH_2(^1A_1)$, and C_2H concentrations, all normalized to the CH_4-free conditions. The somewhat larger reduction of $[C_2H]$ as compared to $[CH(X^2\Pi)]$ is due to the $C_2H + CH_4$ reaction. It can be seen that the experimental relative [CH*] agrees very well with the calculated $[CH(A^2\Delta)]$. Moreover, the data demonstrate that [CH*] correlates with $[CH(X^2\Pi)]$ rather than with $[CH_2(^1A_1)]$; the concentration of singlet CH_2 decreases much less steeply upon CH_4 addition because it is already very rapidly deactivated by collisions with the bath gas atoms.[14,30] Therefore, the present results on CH* are fully consistent with the reaction sequence

$$CH(X^2\Pi) \xrightarrow{C_2H_2} C_3H_2 \xrightarrow{O} C_2H \xrightarrow{O} CH^*$$

and hence confirm that this mechanism is the dominant C_2H source[14] in C_2H_2/O/H systems.

Discussion

As stated above, the measured vertical IP of 11.7 ± 0.4 eV indicates that the C_2H monitored in the C_2H_2/O/H systems is the X $^2\Sigma^+$ state. However, because of the error margin of ±0.4 eV, the IP is not incompatible with the $C_2H(A^2\Pi)$ state, which lies only 10.5 kcal/mol above the ground state. Yet, the k_{2a} value of $1.1^{+1.1}_{-0.5} \times 10^{-11}$ cm^3 molecule^{-1} s^{-1} at T = 290 K of this work is in fair agreement with the $k_{2a} = (1.8 \pm 0.7) \times 10^{-11}$ result that we obtained earlier[11] in a pulse laser photolysis/chemiluminescence study where the C_2H was in its ground state, beyond reasonable doubt. This supports our assignment of the X $^2\Sigma^+$ state to the C_2H in the C_2H_2/O/H systems.

As already emphasized in the earlier work,[11] the rate constant for the CH*-forming channel is surprisingly high, considering that it must compete with much more exoergic channels, producing $CH(X^2\Pi) + CO$ and $C_2O(X^3\Sigma^-$ or $a^1\Delta) + H$. In the earlier work, we offered a tentative rationalization,[11] in which it is assumed that ground electronic state HCCO is the common intermediate of all channels. Its very high energy content will bring the vibrating HCCO above the potential energy well of the bent $^2A''$ equilibrium structure, such that the (anharmonic) bending vibrations will be symmetric about the linear $^2\Pi$ structure, and hence also doubly degenerate. The resulting appreciable nuclear momentum about the molecular axis may couple to the electronic angular momentum by the Renner−Teller effect and thus induce a high Λ. In this way, products with a high electronic angular momentum would be favored. The two highest-Λ product states, satisfying the energy and spin constraints, are $C_2O(a^1\Delta) + H$ and $CH(A^2\Delta) + CO$. It should be emphasized that this tentative rationalization of an unusually high yield of excited products is only applicable to a highly vibrationally excited initial adduct that makes doubly degenerate

bending motions, implying that it is a fluxating linear structure; moreover this "linear" intermediate should exhibit a sufficiently strong Renner−Teller effect. The importance of vibronic coupling in HCCO is witnessed by the splitting of ∼10 kcal/mol between the $^2A'$ and $^2A''$ components of the $^2\Pi$ state at the $^2A''$ equilibrium geometry.[31]

The k_{2a} value extrapolated to flame temperatures, i.e. $k_{2a} \approx 2 \times 10^{-11}$, is of the magnitude required by Joklik et al. to explain the observed CH* in a hot C_2H_2/O_2 flame by reaction r2a.[8] It is worth noting in passing that the [CH*]/[CH(X)] and [CH*]/[C_2H_2] ratios in our atomic flames, i.e. 10^{-3} and 10^{-7}, respectively, are of the same magnitude as in the 40 Torr high-temperature flame of Joklik et al. Therefore, there is no *a priori* reason to doubt that reaction r2a is an important—if not the dominant—CH* production process in high-temperature hydrocarbon flames in general.

The question then arises how the above can be reconciled with the quasi-constancy of the [CH*]/[C_2(X)][OH(X)] ratio observed in hot C_2H_2/O_2 flames by Bulewicz et al.[3] Grebe and Homann suggested that the [C_2][OH] and [C_2H][O] concentration products in flames may be linked.[7] We propose a linkage via the simultaneous partial equilibria $H_2 + O \leftrightarrow OH + H$ and $C_2H + H \leftrightarrow C_2 + H_2$, or $H_2O + O \leftrightarrow OH + OH$ and $C_2H + OH \leftrightarrow C_2 + H_2O$. The first partial equilibrium of each set is known to be fairly rapidly established in hot flames;[32,33] establishment of the second partial equilibrium is subject to the condition that these reactions occur at a faster rate than the net irreversible removal of C_2H or C_2. Provided that the latter condition is met in the flames of Bulewicz et al., the [C_2][OH]/[C_2H][O] ratio would be equal to the pertaining equilibrium constant—which is only moderately temperature dependent—such that the [C_2][OH] product behaves in the same way as and hence is a direct measure of [C_2H][O].

The intensity of the chemiluminescent CH* emission, I(CH*), has been successfully used as a measure of the rate of burning in turbulent flames.[34,35] The question therefore arises as to the relationship between I(CH*) and the burning rate. Considering that reaction r2a is the dominant CH* source, this relation is quite straightforward: the reaction involves two radicals, one oxidizer-based and the second fuel-derived, and the product of their concentrations will obviously be highest where chain branching and hence also the rate of burning are at a maximum. Of course, this explanation is not exclusively applicable to reaction r2a as source of CH*.

Conclusions

In this work, we have established directly and conclusively that the CH* chemiluminescence in C_2H_2/O/H atomic flames is indeed caused by the reaction between C_2H radicals and O atoms.

The rate constant of the $CH(A^2\Delta, v' = 0)$-producing channel in the $T = 300-1000$ K range was determined to be $k_{2a} = 2.4 \times 10^{-11} \exp[-230/T(\mathrm{K})]$ cm^3 molecule^{-1} s^{-1}, with a probable systematic error of a factor of 2. The value found at 290 K, $k_{2a} = 1.1 \times 10^{-11}$, agrees with the result that we obtained very recently in an independent PLP/CL experiment,[11] using entirely different techniques.

It could be shown that the observed effects of CH_4 addition on the CH* chemiluminescence intensity are quantitatively consistent with the C_2H formation mechanism in C_2H_2/O/H systems that we established earlier.[14]

Given the high value of k_{2a}—of the correct magnitude required to explain the high rate of CH* formation observed[8] in hot acetylene/oxygen flames—it is concluded that reaction channel r2a is a major if not the dominant CH* source also in normal hydrocarbon flames. It is argued that the correlation observed by earlier workers between the CH* emission intensity and the [C_2][OH] concentration product[3] might be due to partial equilibria of fast reversible radical reactions linking the above product to [C_2H][O].

Acknowledgment. This research was supported by the Commission of the European Communities (Science Programme, Contract SC1* CT91-0637) and by the Belgian Fund for Scientific Research (Contract NFWO 1.5437.92 N).

References and Notes

(1) Bass, A. M.; Broida, H. P. *NBS Monogr. (U.S.)* **1961**, 24.
(2) (a) Gaydon, A. G.; Wolfhard, H. G. *Flames*, Chapman and Hall: London, 1960. (b) Gaydon, A. G. *The Spectroscopy of Flames*, 2nd ed.; Chapman and Hall: London, 1974.
(3) Bulewicz, E. M.; Padley, P. J.; Smith, R. E. *Proc. R. Soc. London* **1970**, *315*, 129.
(4) Brenig, H. H., Ph.D. Thesis, Wuppertal, 1981.
(5) Glass, G. P.; Kistiakowsky, G. B.; Michael, J. V.; Niki, H. *Symp. (Int.) Combust. [Proc.]* **1965**, *10*, 513.
(6) Brennen, W.; Carrington, T. *J. Chem. Phys.* **1967**, *46*, 7.
(7) Grebe, J.; Homann, K. H. *Ber. Bunsen-Ges. Phys. Chem.* **1982**, *86*, 587.
(8) Joklik, R. G.; Daily, J. W.; Pitz, W. *Symp. (Int.) Combust. [Proc.]* **1986**, *21*, 895.
(9) (a) Renlund, A. M.; Shokoohi, F.; Reisler, H.; Wittig, C. *Chem. Phys. Lett.* **1981**, *84* (2), 293. (b) Renlund, A. M.; Shokoohi, F.; Reisler, H.; Wittig, C. *J. Phys. Chem.* **1982**, *86*, 4165.
(10) Becker, K. H.; Wiesen, P. *Z. Phys. Chem. Neue Folge* **1989**, *161*, 131.
(11) Devriendt, K.; Van Look, H.; Ceursters, B.; Peeters, J. *Chem. Phys. Lett.* **1996**, *261*, 450.
(12) Warnatz, J. *Combust. Sci. Technol.* **1983**, *34*, 177.
(13) Peeters, J.; Van Look, H.; Ceursters, B. *J. Phys. Chem.* **1996**, *100*, 15124.
(14) Boullart, W.; Devriendt, K.; Borms, R.; Peeters, J. *J. Phys. Chem.* **1996**, *100*, 998.
(15) Vinckier, C.; Debruyn, W. *Symp. (Int.) Combust. [Proc.]* **1979**, *17*, 623.
(16) Becker, K. H.; Brenig, H. H.; Tatarczyk, T. *Chem. Phys. Lett.* **1980**, *71*, 242.
(17) Bauer, W.; Engelhardt, B.; Wiesen, P.; Becker, K. H. *Chem. Phys. Lett.* **1989**, *158*, 321.
(18) Luque, J.; Crosley, D. R. *J. Chem. Phys.* **1996**, *104* (2), 2146.
(19) Van Look, H.; Peeters, J. *J. Phys. Chem.* **1995**, *99*, 16284.
(20) Opansky, B. J.; Seakins, P. W.; Pedersen, J. O. P.; Leone, S. R. *J. Phys. Chem.* **1993**, *97*, 8583.
(21) Fontijn, A.; Meyer, C. B.; Schiff, H. I. *J. Chem. Phys.* **1964**, *40*, 64.
(22) Butler, J. E.; Fleming, J. W.; Goss, L. P.; Lin, M. C. *Chem. Phys.* **1981**, *56*, 355.
(23) Langford, A. O.; Petek, H.; Moore, C. B. *J. Chem. Phys.* **1983**, *78*, 6650.
(24) Ashfold, M. N. R.; Fullstone, M. A.; Hancock, G.; Ketley, G. W. *Chem. Phys.* **1981**, *55*, 245.
(25) Böhland, T.; Temps, F.; Wagner, H. Gg. *Ber. Bunsen-Ges. Phys. Chem.* **1985**, *89*, 1013.
(26) Berman, M. R.; Lin, M. C. *Chem. Phys.* **1983**, *82*, 435.
(27) Anderson, S. M.; Freedman, A.; Kolb, C. E. *J. Phys. Chem.* **1987**, *91*, 6272.
(28) Peeters, J.; Langhans, I.; Boullart, W. *Int. J. Chem. Kinet.* **1994**, *26*, 869.
(29) Lander, D. R.; Unfried, K. G.; Glass, G. P.; Curl, R. F. *J. Phys. Chem.* **1990**, *94*, 7759.
(30) Peeters, J.; Devriendt, K. *Symp. (Int.) Combust. [Proc.]*, in press.
(31) Nguyen, M. T.; Boullart, W.; Peeters, J. *J. Phys. Chem.* **1994**, *98*, 8030.
(32) Peeters, J.; Mahnen, G. *Symp. (Int.) Combust. [Proc.]* **1973**, *14*, 133.
(33) Biordi, J. C.; Lazzara, C. P.; Papp, J. F. *Symp. (Int.) Combust. [Proc.]* **1975**, *15*, 917.
(34) Hurle, I. R.; Price, R. B.; Sugden, T. M.. Thomas, A. *Proc. R. Soc. London* **1968**, *A303*, 409.
(35) Abdel-Gayed, R. G.; Al-Khishali, K. J.; Bradley, D. *Proc. R. Soc. London* **1984**, *A391*, 393.